R.M. Wambua et al., Int. Journal of Design & Nature. Vol. 3, No. 4 (2009) 281–295

CLASSIFICATION OF CATCHMENT RISK AREAS USING SPATIALLY DISTRIBUTED EVENT-BASED SOIL EROSION: A CASE OF UPPER NJORO RIVER CATCHMENT, KENYA

R.M. WAMBUA, B.M. MUTUA, D.M. NYAANGA & P.M. KUNDU
Department of Agricultural Engineering, Egerton University, Egerton, Kenya.

ABSTRACT

Human-induced soil erosion and drastic change in land use practices have adversely influenced the land degradation and surface runoff response in upper Njoro River catchment. The drainage area is approximately 127 km^2. Due to human activities, the land has been exposed to accelerated erosion and low land productivity, water scarcity, decline in ground water recharge, siltation of Lake Nakuru and other sediment sinks. This study was conducted to establish event-based risk areas for prioritized conservation within the catchment. Spatially distributed soil erosion map was created as a ratio of sediment yield to sediment delivery ratio (SDR). Modified Universal Soil Loss Equation (MUSLE) integrated within a Geographical Information Systems environment was used to create the sediment yield map. Spatial data layers for the MUSLE were derived from a 20-m resolution Digital Elevation Model, soil property, land use maps and climatic data of the catchment. Land use map was derived from Landsat imagery via its processing using Integrated Land and Water Information Systems software. The results show that the spatially distributed soil erosion ranged from 0.06 to 0.51 t/ha for a 43.2-mm rainfall event. Spatially distributed SDR ranged from 0.09 to 0.82, while the average SDR for the whole catchment was 0.72. These values were derived using an empirical equation. A new contribution was made by developing spatially distributed slope length factor, SDR, runoff volumes, MUSLE parameters and classified erosion risk areas for prioritized catchment conservation. This means that the event-based soil erosion classification can be adopted for prioritized soil and water conservation within Njoro catchment.

Keywords: accelerated erosion, GIS, MUSLE, Njoro, prioritized conservation, water scarcity.

1 INTRODUCTION

Soil erosion due to surface runoff has caused tremendous land degradation on the upper Njoro River catchment. The erosion has led to low land productivity, while the runoff has resulted in decline in water supply due to decrease in ground water recharge, pollution and siltation of Lake Nakuru. Flow rate in the Njoro River has been declining over time leading to water scarcity in the area. Urgent and appropriate planning, conservation and management of land and water resources are required. To accomplish this task, data on spatially distributed soil erosion within the catch ment are essential. Identification of erosion risk areas for conservation planning is necessary. This requires erosion baseline data on a spatial domain. However, such data for the upper Njoro catchment is scanty.

Catchments experience critical natural resource degradation at different rates and different points [1, 2]. This resource degradation varies as a result of geomorphological heterogeneity of most of the catchments such as Njoro. It has been noted that the degradation processes of catchments are complex and associated with variation in spatially distributed soil erosion, surface runoff and sediment yield [3]. This has been attributed to ever-changing surface runoff, as influenced by changing land use practices on specific locations within catchments [4]. To better understand hydrological processes, land and water resources degradation within catchments, a spatially distributed approach should be used in their study [5]. The water erosion on any catchment beginsas a result of raindrop impact on the surface [6, 7, 8, 9]. As the rainfall progresses, sheet, rill and gulley erosion develop from the runoff [10, 11, 12,]. Once the soil particles have been detached, they are then transported by surface

ISSN: 1755-7437 (paper format), ISSN: 1755-7445 (online), http://journals.witpress.com
DOI: 10.2495/D&NE-V3-N4-281-295

runoff down slope and deposited at various points called sinks [13, 14]. This forms the bases of land and water resources degradation.

Njoro River catchment has experienced drastic land use changes since 1970. Rapid forest reduction has been noted since 2000 and 2003 in the upper Njoro River catchment [15, 16]. Currently, the area occupied by the forest is approximately 21% [17]. Intensive cultivation on the catchment affected the erosion and surface runoff dynamics in Njoro River catchment. Due to human-induced soil erosion within rural catchments, many sectors in Kenya are facing serious water shortage. This has been attributed to changes in hydrologic response of catchments over time [18, 19]. Integrated catchment planning, management, design of hydraulic structures and conservation of land and surface water resources require statistics of spatially distributed soil erosion and runoff [20]. This study attempts to provide data on such issues for the case of Njoro catchment.

Hydrological and soil erosion studies have recently received new outlook with the development and application of remote sensing (RS) techniques. For instance, Barkhordari [21] and Baldyga [15] ascertained the use of this technique in monitoring hydrologic response of Minab and Njoro catchments, respectively, to land use transformations. Another tool that has been used in hydrological modeling is the Geographical Information Systems (GIS) [22, 23, 24]. This is a combination of organized computer system and geographical data designed to efficiently capture, store, update, manipulate, analyze and display all forms of geo-referenced data [25]. The RS and GIS tools are important in the field of hydrology and water resources development. Hydrological modeling involves huge amounts of spatial data management and thus an efficient system such as GIS to handle the data is needed.

The study presented here was undertaken with a main objective of classifying risk areas within upper Njoro catchment for prioritized conservation using spatially distributed event-based soil erosion through sediment modeling in conjunction with RS and GIS.

2 MATERIALS AND METHODS

2.1 Study area

The upper Njoro River catchment is approximately 127 km^2. This study area lies between latitudes 0°15′S and 0°25′S and longitudes 35°50′E and 36°05′E (Fig. 1). The area has a bimodal-distributed rainfall pattern averaging 1150mm annually. Precipitation peaks in May and October. The catchment exhibits various soil types [26]. The lower part of the catchment consists of erosive and lucustrine soils, while the upper part is predominantly loamy.

2.2 Estimation of spatially distributed event-based sediment yield

The Modified Universal Soil Loss Erosion (MUSLE) model was adopted for sediment yield estimation within the catchment. On a spatial domain, this model is expressed as

$$Y_i = a(Q_i q_{pi})^b K_i L_i S_i C_i P_i, \tag{1}$$

where each cell is represented by i. Y_i is the sediment yield from an individual storm (tones), Q_i is the runoff volume (m^3), q_{pi} is the peak runoff rate (m^{3}s^{-1}) and K_i, L_i, S_i, C_i and P_i are the RUSLE factors. The parameters a and b are empirical values that may vary for different catchments. For the United States catchments, the values for a and b are equal to 11.8 and 0.56, respectively. However, for many catchments in Africa the values of a and b should be determined through calibration and validation.

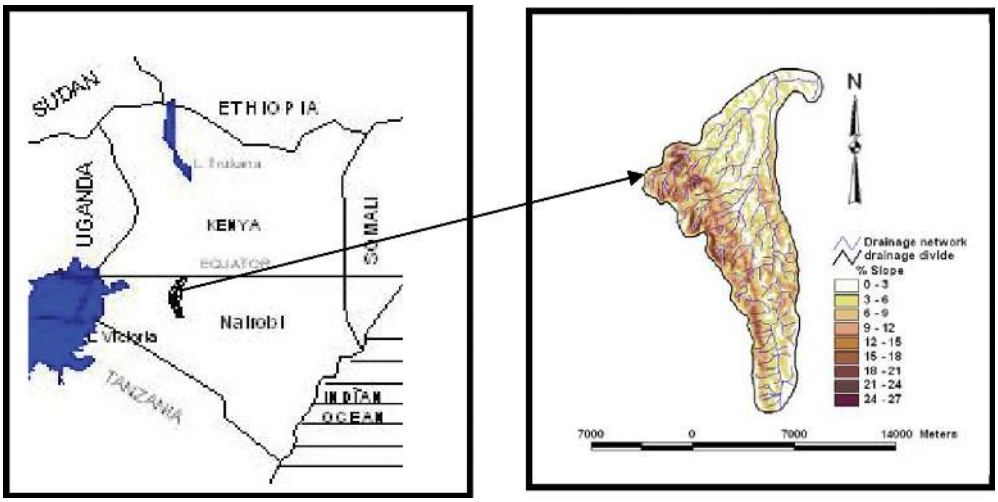

Figure 1: Map of Kenya showing upper Njoro River catchment.

To measure sediment and runoff at the catchment outlet, sediment was sampled after every event, while the runoff was determined at the gauged station using rating equation. The sediment yield and runoff were taken for 32 rainfall data events. The MUSLE model results were calibrated automatically by selecting a first 16 set of data from the total. The catchment empirical parameters a and b of the MUSLE and the Nash–Sutcliffe coefficient [27] were optimized based on the observed sediment yield for each event. The Nash coefficient is expressed as

$$R^2 = 1 - \frac{\sum_{i=1}^{n} (S_o - S_s)^2}{\sum_{i=1}^{n} (S_o - S_m)^2}, \tag{2}$$

where R^2 is the Nash–Sutcliffe coefficient, S_o S_s and S_m are the observed, simulated and observed mean values, respectively, while n is the number of observations. The conditions for the coefficient are that the R^2 values range from negative to one. If the values of R^2 lie between zero and one, then the model predictive ability is effective. The values of one indicate a perfect relationship between the simulated and observed values. However, if R^2 is equal to zero, then there is no relationship between the simulated and measured values and thus no need of using average event values as a representative for that particular event [28].

The optimum values of a and b that gave the maximum Nash–Sutcliffe coefficient and sediment yield that compared accurately with the observed values were considered to be acceptable for the upper Njoro catchment. The sediment yield values for the remaining set of data were validated simultaneously with the calibration through optimization technique. The optimum values for a and b were 11.6 and 0.58, respectively. Thus, the MUSLE developed for upper Njoro River catchment is of the form:

$$Y_i = 11.6(Q_i q_{pi})^{0.58} K_i L_i S_i C_i P_i. \tag{3}$$

2.3 Estimation of spatially distributed runoff

For improved spatial parameter estimation, efforts have been done to develop the performance of existing hydrological models. The modified curve number (CN) approach was used to estimate runoff in a spatial domain. The resulting equation can be used to determine the runoff from rough fields more accurately than the original equation [29]. This is done by introducing random surface parameter for area of interest as per the Limburg Soil Erosion Model. The equation is expressed as

$$Q_i = \frac{(P_i - 0.2S_i)^2}{P_i + 0.8S_i} - \Phi_i, \quad P > (0.2S_i - \Phi_i), \tag{4a}$$

$$Q_i = 0, \quad P < (0.2S_i - \Phi_i). \tag{4b}$$

The subscript i is the ith cell and Q_i is the accumulated runoff depth (mm), P_i is the accumulated precipitation (mm) and Φ is depression storage. The S_i is the maximum soil water retention parameter (mm) computed from the equation:

$$S_i = \frac{25400}{CN_i} - 254, \tag{5}$$

where CN_i is the curve number which is based on hydrologic response unit (HRU). The SCS HRU is based on the soil infiltration or runoff potential. The spatial CN map was created by processing the land use map of the study area using Integrated Land and Water Information Systems (ILWIS) and assigning CN within the GIS environment based on HRU (Fig. 2).

Depression storage was determined based on the equation [4]

$$\Phi_i = 0.112R_i + 0.31R_i^2 - 0.012R_iSg_i, \tag{6}$$

where R is the random roughness (cm) and Sg_i is the slope gradient (%). The random roughness values were assigned depending upon the field operations based on a field survey. The parameters were then combined using the map calculator extension of the GIS to give runoff depth results. The runoff volume results were obtained by converting the depth into meters and then multiplying by the spatial area map.

2.4 Peak runoff rate

The peak flow rate was determined using a function first developed and used in erosion productivity impact calculator (EPIC) model [30, 4]; the peak flow rate is expressed as

$$q_{pi} = 3.97A_i^{0.717}S^{0.16}\left(\frac{Q_i}{25.4}\right)^{0.903A^{0.017}} LW^{-0.19}, \tag{7}$$

where q_{pi} is peak runoff rate ($m^3\ s^{-1}$), A_i is the cell area (km^2), S is the gradient of channel along flow slope (m/km), Q_i is the runoff depth (mm) and LW is the length to width ratio of the cell which depends upon the resolution of the Digital Elevation Model (DEM) used. The DEM was created by digitizing the contours of topographic map of the study area. The digitized contours were then converted into Grid format within the ArcView GIS which was subsequently corrected to yield a corrected DEM (Fig. 3a). The S_i was established by converting the percent slope map (Fig. 3b) into units of m/km within GIS environment.

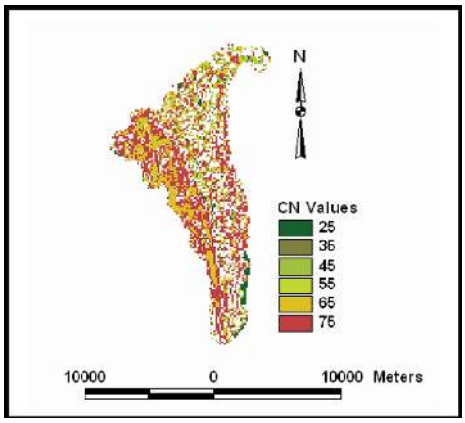

Figure 2: Spatial CN factor value.

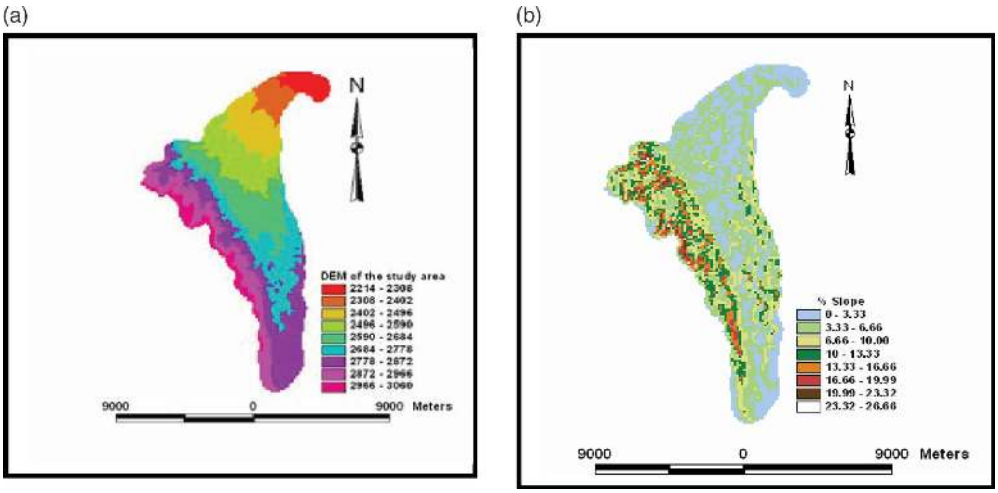

Figure 3: (a) The DEM and (b) variation of slope within the study area.

2.5 Determination of spatially distributed slope length (LS) factor

The MUSLE slope length (LS) factor was derived from the generated DEM (Fig. 3a) of the study area. The LS factor at any point $r(x, y)$ on a hill slope was computed from continuous equation [5] using ArcView software via map calculation. The equation is in the form:

$$LS = \left(\frac{A}{22.13}\right)^{0.4} \times \left(\frac{\sin\Theta}{0.0896}\right)^{1.3}, \tag{8}$$

where A is the upslope contributing area (m^2) and Θ is the slope (degrees). An upper bound for this equation is 122m. This means that the runoff becomes concentrated for any LS greater than 122m. The DEM which was based on a 20-m resolution grid was used to determine the percentage slope.

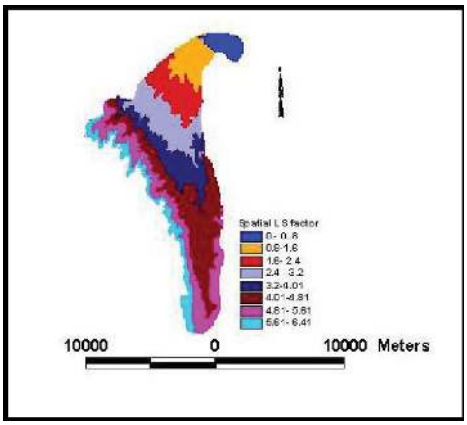

Figure 4: Spatially distributed LS factor values within upper Njoro River catchment.

This was used to prepare thematic map of spatial LS factors (Fig. 4) based on eqn. (8) using map calculator of ArcView GIS.

The results of spatial LS factor values within the upper Njoro catchment was mapped over the catchment.

2.6 Crop management, soil erodibility and conservation practice factors

The MUSLE C-factor is a combination of subfactors that correspond to surface cover, surface roughness, canopy cover and previous land use practice [31]. To establish the spatial C-factor for the Njoro catchment, a multispectral remote data from Landsat ETM of 2007 was used to derive information on land use. This image was then processed using ILWIS software.

The major land use types were identified, classified and then their associated C-factor values assigned for every land use type based on points taken with the aid of a Global Positioning System during field surveys of the study area. C-factor values for Njoro catchment for each land use were assigned (Table 1). The crop management factor value is the ratio of soil loss under a given crop to the soil loss of the same land when bare. The K-factor is a function of soil particle distribution within the soil. This comprises the percentage of silt and coarse sand, organic matter, soil structure and permeability. A soil polygon layer for the study area was delineated and erodibility values assigned (Table 1). The polygon layer was then converted into a grid using the poly-grid command. The resolution of the resulting soil property map was assumed to match that of the K-values. Soil properties map was converted into hydrological soil group grid and then overlaid with land use grid layer to derive the CN grid (Fig. 2). The CNs were then assigned to various HRUs based on the land use and hydrologic soil group through a rule-based approach by considering crop type and field surface conditions [31].

2.7 Estimation of spatially distributed event-based soil erosion

The identification of erosion risk areas required data on spatial distribution of erosion within the study area. To derive this, it was necessary to first determine the spatial distribution of sediment delivery ratio (SDR). A function that relates the catchment characteristics to the SDR gives more accurate values than most empirical models. Such a function has been developed and applied in many areas [32].

Table 1: The C- and K-factor values for different land use types.

Land use	C-factor values	K-factor values
Settlement	0.320	0.150
Forest	0.038	0.035
Agriculture	0.350	0.290
Shrubs	0.088	0.090
Grassland	0.092	0.095

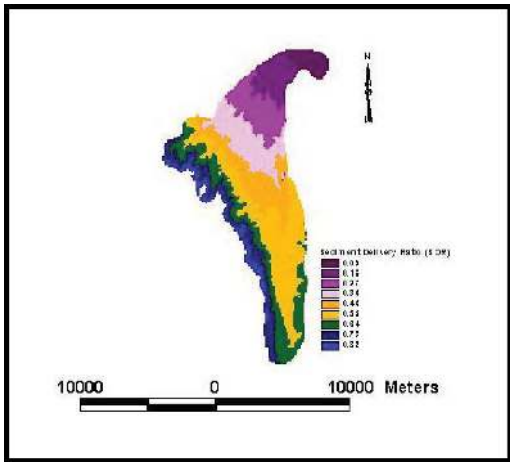

Figure 5: Spatially distributed SDR within the upper Njoro River catchment.

Table 2: The prioritized soil and water conservation for a 42.3-mm rainfall event.

Soil erosion range (t/ha)	Erosion category/class	Conservation priority
0–0.06	Too low	8
0.06–0.13	Very low	7
0.13–0.19	Low	6
0.19–0.26	Moderate	5
0.26–0.32	High	4
0.32–0.38	Very high	3
0.38–0.45	Too high	2
0.45–0.52	Extremely high	1

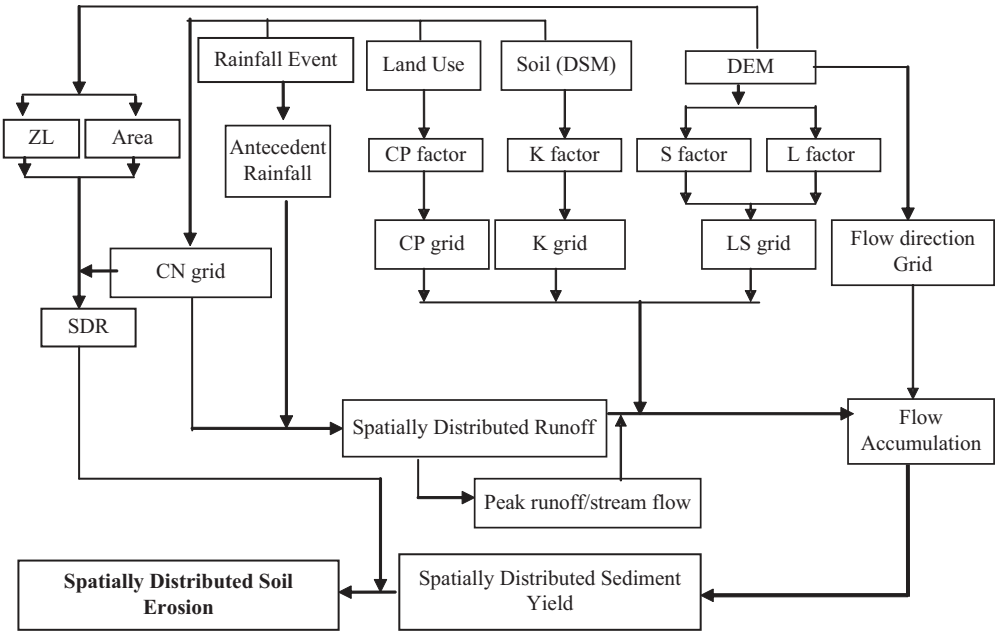

Figure 6: Flow chart of the integration of the steps involved.

The function relates SDR with drainage area, relief length ratio and the CN. The equation is summarized in the form:

$$SDR = 1.366\times10^{-11}(A)^{-0.0998}(ZL)^{0.3629}(CN)^{5.444}, \quad (9)$$

where A is the drainage area (km^2), ZL is the relief length ratio (m/km) and CN is the average SCS CN (dimensionless).The A, ZL and CN grids were manipulated as per eqn. (9) carried out using the Map calculator of the ArcView GIS. The results of the SDR_i were obtained (Fig. 5).

The resulting spatial SDR grid was the multiplied by the spatial distribution of the sediment yield to give spatial distribution of erosion (Fig. 12).

2.8 Classification erosion risk areas

To prioritize the conservation within the catchment, the soil erosion was categorized into eight classes. The critical areas that need urgent soil and water conservation were clearly identified from the map. The highest event-based soil erosion class was assigned conservation priority code one (Table 2). The conservation event-based priority codes were plotted against erosion (Fig. 12). The method used was summarized in flow chart (Fig. 6).

3 RESULTS AND DISCUSSION

3.1 Spatially distributed event-based surface runoff

The modified CN method was used to determine spatially distributed surface runoff depth. The runoff was converted into spatially distributed runoff volume as a product of the runoff depth and area. This was achieved via application of map calculator extension of the Arc GIS to develop a spatial runoff volume layer (Fig. 7).

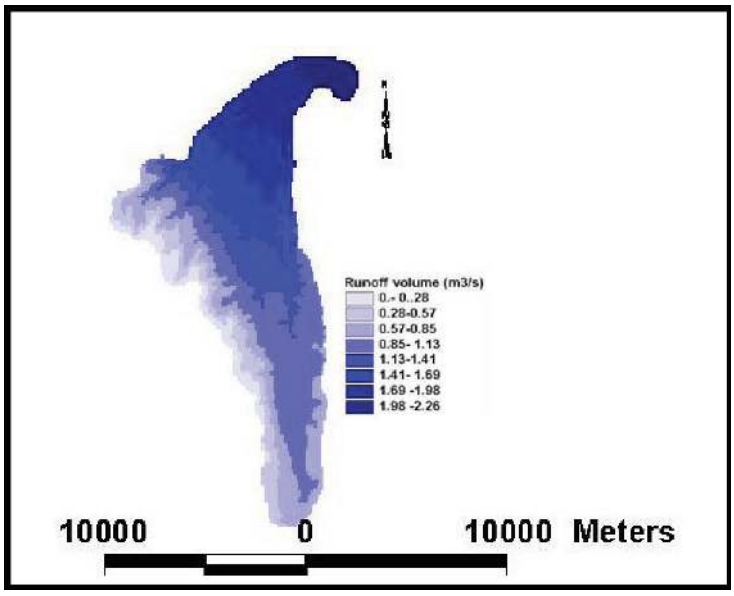

Figure 7: Spatially distributed runoff volume for the 42.3-mm rainfall event.

The spatial CN values shape file (Fig. 2) was developed as an input parameter in determination of spatial runoff. The CN values for upper Njoro catchment ranged from 25 to 75. The values were assigned to each HRU to indicate the corresponding runoff potential. The HRU consist of a combination of land use or treatment class, hydrologic and soil groups [33, 31]. The soil erodibility K-factor value shape file created for the catchment gave values ranging from 0.090 to 0.290. The K-factor was expressed as a function of percent silt and course sand, soil permeability, soil structure and percent organic matter. This is best represented in soil nomograph which was used in assigning K-values [7].

Although the spatially distributed runoff volume is greatly influenced by the event magnitude, it was also found to vary with slope. For the upper Njoro catchment, the highest and lowest values were found to range from 1.98 to 2.26 and 0 to 0.28 m^3 for a 42.3-mm rainfall event. These values occurred within the slopes of 27% and 3%, respectively.

The results show a logarithmic relationship between the surface runoff volume and rainfall magnitude. Based on the spatially distributed runoff volume map, the lowest values ranged from 0 to 0.28 m^3s^{-1} and the highest values ranges from 1.98 to 2.26 m^3s^{-1} for a 42.3-mm rainfall event. From the results, spatial peak flow rate was directly proportional to the event magnitude. The highest range was 107–121 m^3s^{-1} and 126–142 m^3s^{-1} for the 42.3- and 75.5-mm rainfall events, respectively. The lowest values of spatial peak flow rate ranged from 0 to 13 and 0 to 16 m^3s^{-1} for the respective rainfall events (Fig. 8).

3.2 Spatially distributed event-based sediment yield

Spatially distributed sediment yield was examined using the MUSLE for upper Njoro catchment (eqn. (3)) within GIS environment. The MUSLE parameters were integrated using the map calculator extension of the ArcView GIS. The results showed variation of sediment yield for different events.

A 42.3-mm rainfall event produced a maximum sediment yield range of 0.0027–0.0041 t/ha, while the 75.5-mm event gave 0.046–0.051 t/ha. The maximum values were realized at the upper

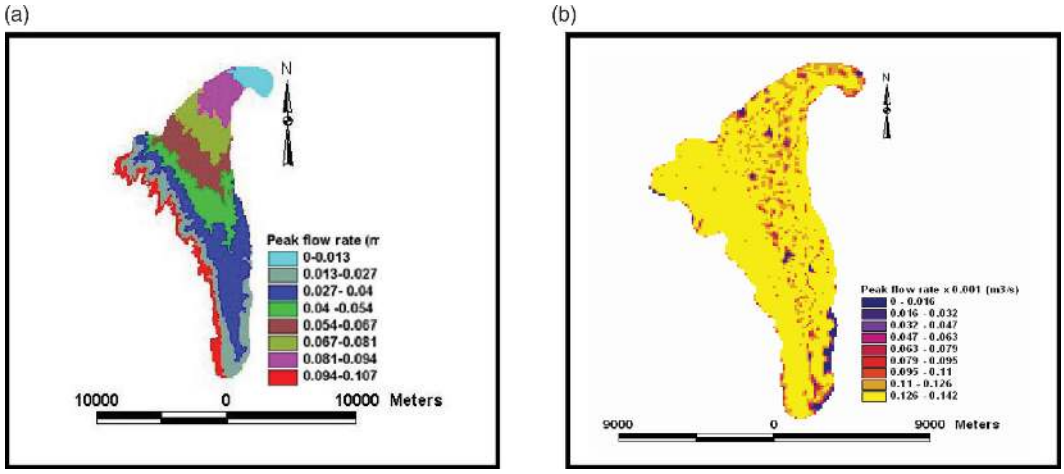

Figure 8 : Spatially distributed peak runoff rates for a (a) 42.3- and (b) 75.5-mm rainfall event, respectively.

regions of the catchment where slope is steep ranging from 22% to 26%. The minimum range of sediment yield values for the two events were 0–0.005 and 0–0.006 t/ha. These values were realized at the lower regions of the catchment where slopes are a bit gentle ranging between 0% and 3%. It was possible to plot the sediment yield against the peak runoff rate at the outlet of the catchment (Fig. 9).

It was found that the two were positively correlated with correlation coefficient values of 0.65 and 0.58 for the two gauged stations. Based on the runoff rate, the sediment yield rating equation was developed for these stations (Fig. 9). The spatial distributions of some selected storms were also determined.

3.3 Spatial variation of SDR

Determination of spatially distributed soil erosion required the spatial distribution of both sediment yield and SDR. The SDR was established as described earlier and the results were mapped over the study area (Fig. 10).

3.4 Spatially distributed soil erosion

Based on the spatial SDR and spatial sediment yield results above, the spatial soil erosion for the 26.0- and 42.3-mm events (Fig. 11) was determined using the map calculator of the ArcView. The overall SDR of 0.72 and 0.87 were determined using eqn. 9 for the 127- and 110-km^2 catchment area for the Treetop and Egerton stations. This was based on an average relief length ratio of 11 m/km and average CN of 55 via the ArcView.

The highest and lowest spatial distribution of soil erosion for a 42.3-mm rainfall events were 0.45–0.51 and 0–0.06 t/ha, respectively. For a 26.0-mm event, these values were found to be 0.25–0.286 and 0–0.036 t/ha. The values were based on the spatial distribution of SDR for the catchment which ranged from to 0.09 to 0.82 with overall catchment SDR values of 0.72 and 0.87 as derived from the area, relief length ratio and CN method for the areas draining to the Egerton and Treetop stations, respectively. It was found that the sediment yield increased with the event magnitude. However, the sediment

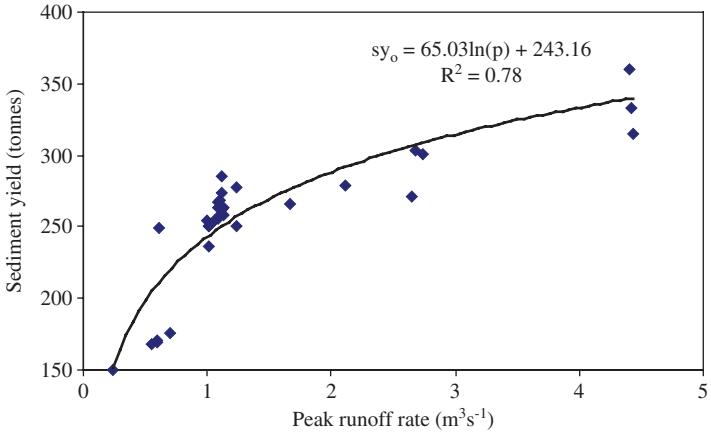

Figure 9: The observed sediment yield versus runoff rate at catchment outlet.

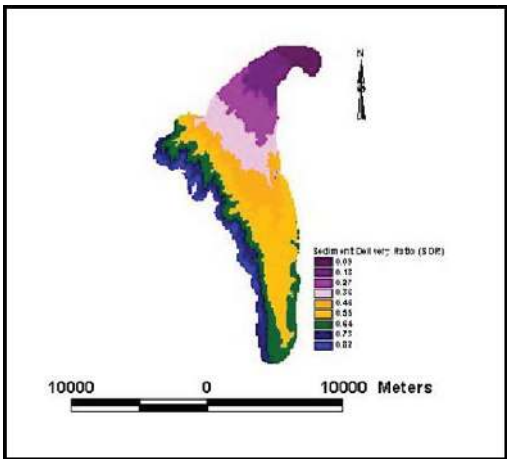

Figure 10: Spatial variation of SDR within the upper Njoro River catchment.

yield was found to increase successively from subcatchments 6, 7 and 8. The subcatchment 8 is mainly settlement area, while 6 and 7 are predominantly agricultural lands. The soil erosion was categorized into eight classes. The critical areas that need urgent soil and water conservation are clearly identified from the map (Fig. 12). The highest erosion was classified as extremely high, while the lowest was categorized as too low. Conservation priority codes were also assigned priority (Table 2).

3.5 Prioritization of conservation based on soil erosion

The results of the plot can be used in identification of the spatial event-based erosion level. The erosion levels vary with the rainfall magnitude. The higher the rainfall magnitude, the higher the erosion level for the same conservation priority. For instance, the rainfall magnitudes of 75.5, 43.2, 26.0 and 15.1 mm resulted into erosion magnitudes of 0.85, 0.48, 0.3 and 0.15 t/ha, respectively.

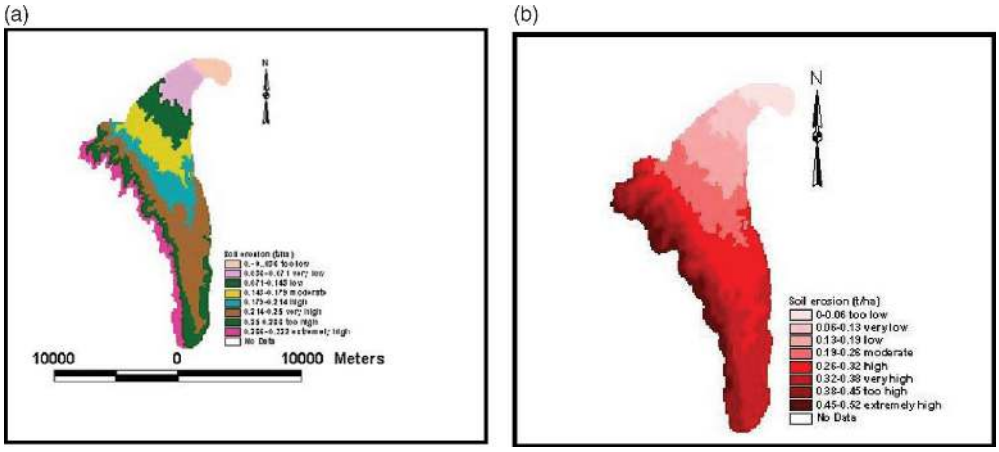

Figure 11 : Spatially distributed soil erosion within upper Njoro catchment for a (a) 26.0- and (b) 42.3-mm rainfall event, respectively.

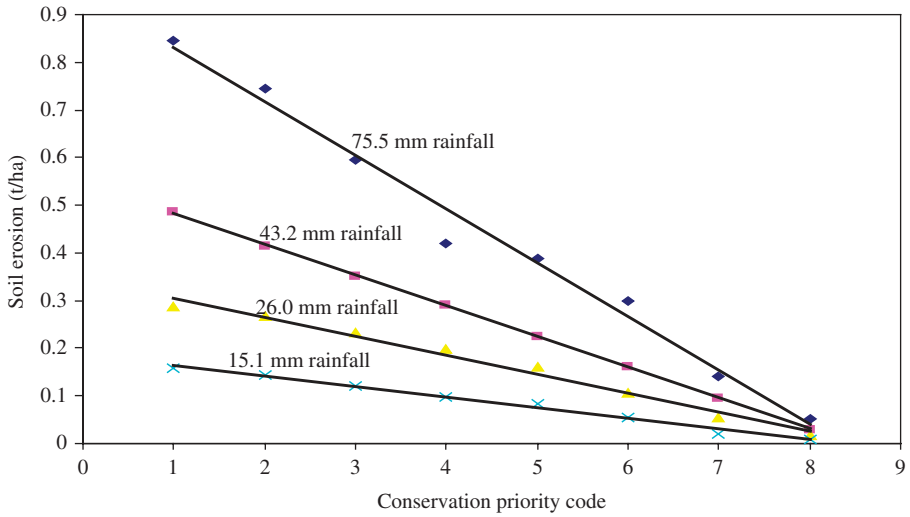

Figure 12: Conservation priority graph codes for different event magnitudes.

3.6 Sensitivity analysis

Surface runoff estimation is vital in strategic planning, management and conservation of surface runoff and soil erosion from catchments. In this connection, quantifying modified SCS CN method sensitivity (Fig. 13) to parameter changes help to understand its response to errors in parameter estimation.

Sensitivity analysis was performed for an average event of 17.2 mm within the study period. All the influencing factors in the model were tested. The predicted peak runoff and runoff volume considered for the sensitivity analysis were 38.08 m^3s^{-1} and 0.64 m^3, respectively. The parameter values under grid cell were uniformly altered at equal intervals of 5%. The maximum and minimum alterations were 50% and −50%. Results of the sensitivity analysis showed that the CN estimation will produce

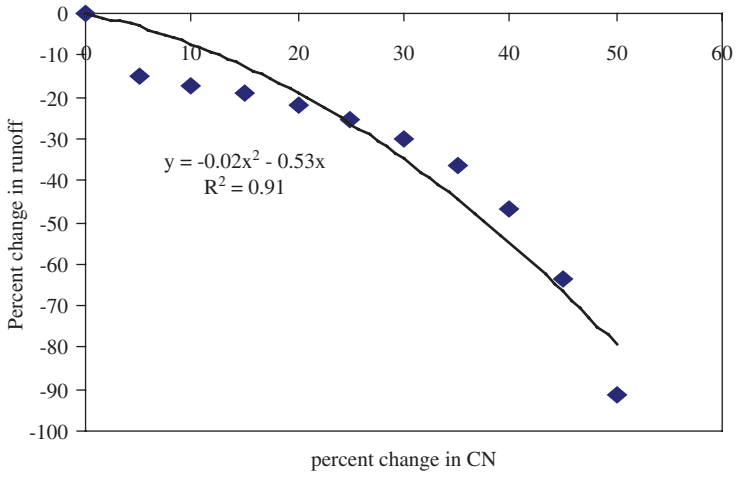

Figure 13: The effect of increasing CN on the runoff.

significant effect on the runoff results. The peak runoff was more sensitive to an increase in CN than a decrease. It was noted that an increase of 50% in CN produced a decrease in peak runoff of 91.4%, whereas a decrease of 50% led to an increase of 9.8%. Variation of LS factor by ±50% was found to change the peak runoff rate by ±5%. The baseline depression storage considered in this study was 6 mm. A change of depression storage by 50% resulted into a -27.06%, while a decrease gave –4.97%. The other parameters resulted into smaller values. The analysis show that CN is the most sensitive parameter followed by depression storage. Thus, significant caution was necessary while estimating these sensitive parameters.

4 CONCLUSION AND RECOMMENDATIONS

From the study, event-based spatially distributed soil erosion was used to assign catchment conservation codes. The respective codes and event magnitudes were used to create graphs for prioritized catchment conservation. A new contribution in this work is the creation of prioritized conservation options of Njoro catchment, spatially distributed SDR and LS factors of the catchment. The spatially distributed SDR and LS factors for Njoro catchment ranged from 0.09 to 0.82 and 0-0.8-6.41, respectively. The MUSLE was integrated within the GIS environment and parameters were determined through the optimization technique. The sensitivity analysis showed that CN is the most sensitive parameter in modified CN method used in the estimation of runoff volume.

Further research in the following aspects of runoff needed for a better understanding and improvement of the concluded work. A wider research on spatially distributed soil erosion and runoff rate, within the upper Njoro catchment, should be carried out. Such a study should be based on temporal and spatial data for a number of years using numerous gauged stations for sediment and runoff monitoring. More accurate monitoring techniques of the sediment, runoff and rainfall for erosion and runoff modeling are recommended through establishment of more gauged stations within the catchment.

ACKNOWLEDGEMENTS

The authors acknowledge the Division of Research and Extension of Egerton University for the financial support offered for this study. The funds were particularly useful in postgraduate research carried out by the corresponding author. This paper is part of the postgraduate research.

NOMENCLATURE

A_i	Area of subcell *i*
C	Crop management factor
CN_i	CN for cell *i*
K	Soil erodibility factor
L	Length factor
LW	length to width ratio
P_i	Conservation practice factor estimated for cell *i*
P_i	Precipitation per polygon
p_i	Accumulated precipitation estimated for cell *i*
Q_i	Accumulated runoff volume for cell *i*
q_{pi}	Peak flow rate
R	Random roughness
R^2	Nash–Sutcliffe coefficient
S	Gradient of channel along flow path
S	Slope factor
Sg_i	Slope gradient
S_i	Maximum soil retention parameter
Y	Single storm sediment yield
Y_i	Sediment yield from cell *i*
Y_{oi}	Sediment yield for a relatively homogeneous cell *i*
ZL	Relief length ratio
Φ	Depression storage parameter

REFERENCES

[1] UNEP, *Deserts and Desertification World Environment Conference*, Algiers, 3–5 June 2006.
[2] White, B. & Goh, E.K.H., Systematic reliability-based environmental design of the efficient engineered landscape profiling. *J. Envr. Engineering*, **129(7)**, pp. 620–628, 2003.
[3] Palmer, M., Bockstael, J., Morgan, G., Wiegand, C., Ness, K.V. & Pissurto, J., Spatial patterning of land use conversion. *Journal of Hydrologic Engineering*, **7(1)**, pp. 27–34, 2005.
[4] Kandrika, S. & Venkataratnam, L., A spatially distributed event based model to predict sediment yield. *J. Spatial Hydrology*, Spring, **5(1)**, 2005.
[5] Lim, J.K., Sagong, M., Engel, B.A., Tang, Z., Choi, J. & Kim, K., GIS based sediment assessment tool. *J. CATENA*, **64**, pp. 61–80, 2005.
[6] Das, G., *Hydrology and Soil Conservation Engineering*, Prentice-Hall: New Delhi, 2002.
[7] Morgan, R.P.C., *Soil Erosion and Conservation*, John Wiley & Sons, Inc.: New York, 1986.
[8] Morgan, R.P.C., Rickson, R.J., McIntyre, K., Brewer, T.R & Altshul, H.J., Soil erosion of the central part of Swaziland Middleveld. *Journal of Soil Technology*, **11**, pp. 263–289, 1997.
[9] Ongweny, G.S. Kiithia, S.M. & Denga, F.O., *An Overview of Soil Erosion and Sedimentation Problems in Kenya*, eds R.F, Hadly & T. Mizuyama, No. 217 Yokohama, Japan, 1993.
[10] FAO, Guidelines for mapping and measurements of rainfall induced erosion processes, 2005. http://www.fao.org/docrep/X5302e09.htm, accessed on 15 September 2006.
[11] Liu, Q.Q., Chen, L., Li, J.C. & Singh, V.P., Roll waves in overland flow. *Journal of Hydrologic engineering*, **10(2)**, pp. 110–117, 2005.
[12] Raude, J.M., *Determination of Soil Loss and Surface Runoff Under Varying Rainfall Intensity in Different Land Use Practices in the River Njoro Catchment*, MSc Thesis, Department of Agricultural Engineering, Egerton University, 2006.

[13] Schwab, G.O., Fangmeier, D.D., Elliot, W.J. & Frevert, R.K., *Soil and Water Conservation Engineering*, 4th edn, John Willey and Sons Inc.: New York, 1993.
[14] Shaw, E.M., *Hydrology in Practice*, 3rd edn, Chapman & Hall Co.: London, 1994.
[15] Baldyga, T.J., *Assessing Land Cover change Impacts in Kenya's River Njoro Watershed Using Remote Sensing and Hydrologic Modeling*, MSc Thesis, University of Wyoming, 2005.
[16] Gichaba, M., Chivonga, W., Baldyga, T.J. & Miller, S.N., Assessing the impact of land cover change in Kenya using remote sensing and hydrological modelling. *ASPRS Annual Conference Proceedings*, Denver:, Colorado, 2004.
[17] Otieno, H., *Estimation of Direct Runoff and Sediment Yield in the Upper Njoro River Catchment in Kenya*, MSc Thesis, Department of Agricultural Engineering, Egerton University, 2006.
[18] Biamah, E.K., Sharma, T.C. & Stroosnider, L., Simulation of watershed peak runoff rate using the Nash model. *Journal of Engineering in Agriculture and Environment*, **2**, pp. 49–56, 2002.
[19] Li, K.Y., Coe, M.T., Ramankutty, N & De Jong, R., Modeling hydrological impact of land use change in West Africa. *Journal of Hydrology*, No. 337, pp. 258–268, 2007.
[20] Wambua, S.M., Efforts at integrated water resource management, Network for Water and Sanitation (NETWAS), 2002. http://www.netwas.org/newsletter/articles/2002/05/01, accessed on 1 September 2006.
[21] Barkhordari, J., *Accessing the Effect of Land Use Changes on the Hydrologic Regime by RS and GIS*, PhD Thesis, Netherlands, 2003.
[22] Mitasova, H., HofieRka J., Zlocha, M. & Hverson, L.R., Modeling topographic potential for erosion and deposition using GIS. *Journal of GIS*, **10(5)**, pp. 629–641, 1996.
[23] Castillo, V.M., Plaza, G.A. & Mena M.M., The role of antecedent soil water content in the runoff response of semi-arid catchments. *Journal of Hydrology*, **284(1/4)**, pp. 114–130, 2003.
[24] Nurmohamed, R., Naipal, S. & De Smedi, F., Hydrological modeling of the upper Suriname River basin using Wetspa and ArcView GIS. *Journal of Spatial Hydrology*, **1(1)**, pp. 67–88, 2006.
[25] Singh, V.P. & Fiorentino, M. (eds), *Geographical Information Systems in Hydrology*, Springer-Verlag: London, 1996.
[26] Mainuri, Z.G., *Land Use Effects on Spatial Distribution of Soil Aggregate Stability within the River Njoro Watershed*, Kenya, MSc Thesis, Department of Geography, Egerton University, 2005.
[27] Nash, J. & Sutcliffe, J., River rate forecasting through conceptual models. *J. Hydrology*, **10**, pp. 282–290, 1970.
[28] Jetten, V.G., LISEM: a physically-based runoff and erosion model, 2005. http://www.geog.uu.nl/lisem.html, accessed on 11 august 2006.
[29] Williams, J.R., Sediment graph model based on an instantaneous sediment graph. *Journal of Water Resources Research*, **14(4)**, pp. 659–664, 1978.
[30] Haan C.T., Barfield, B.J. & Hayes, J.C., *Design Hydrology and Sedimentology for Small Catchments*, Academic Press: California, USA, 1978.
[31] Williams J.R., Sediment delivery ratios determined with sediment and runoff models, proceedings of symposium on erosion in inland water. *Hydrological Sci*., No. 122, pp 168–179, 1977.
[32] Chow, V.T., Maidment, D.R. & Mays, L.W., *Applied Hydrology*, McGraw-Hill: New York, 1988.
[33] Wiliiams, R.R., Nicks, A.D. & Arnorl, J.G., Simulator of water resources in rural basins. *Journal of Hydraulic Engineering*, **11(6)**, pp. 82–92, 1988.